Improvements to Long-Pulse–System Performance and Operational Efficiency on OMEGA EP

Introduction

An important operational goal of the Omega EP Laser Facility is to provide principal investigators with maximum UV energy on target, while maintaining UV peak fluences within an acceptable margin for safe operation. To optimize the long-pulse, on-target energy of OMEGA EP, we have pursued a threefold effort: (1) improve the laser-induced damage threshold of beam-transport optics; (2) improve the near-field beam profile; and (3) develop simulation tools to use during shot operations that provide rapid prediction of laser-system performance. These simulation tools predict the UV near-field beam-fluence distribution and on-target energy based on measurements of the inputs to the main amplifiers and are regularly used during shot operations. They have streamlined daily system qualification, making it possible for UV energy to be maximized within current system constraints.

Each of the four OMEGA EP beamlines uses a folded architecture and type-I/type-II frequency-conversion crystal (FCC) design based at the National Ignition Facility (NIF), as shown in Figs. 125.37(a) and 125.37(b).[1] Beamlines 1 and 2 can be operated in either short-pulse or long-pulse mode, while Beamlines 3 and 4 are dedicated to long-pulse operation. All beams are amplified in two passes through a 7-disk booster amplifier and four passes through an 11-disk main amplifier. Depending on the required shot conditions, the main amplifier operates with a variable number of pumped disks. Each beamline has an independent front-end laser source that provides a seed pulse that is injected into the transport spatial filter. The seed originates in a single-frequency fiber laser and is amplified in a regenerative amplifier (regen) after temporal shaping to a level of ~5 mJ. Further preamplification is provided by Nd:glass amplifiers prior to injection into the beamline. Spatial beam shaping is accomplished by two different apodizing elements located in the laser sources' front end. The first apodizer is located immediately after the regen and shapes the edges of the beam from round to square. The second apodizer is located just prior to the glass amplification stage and provides precompensation for the roll-off in gain that occurs at the edges of the beamline disk amplifiers.[2] The spatial gain variation of the front-end glass amplifiers is compensated by appropriately sizing the regen Gaussian output beam on the first apodizer.

Table 125.III shows the OMEGA EP individual beamline long-pulse–design energies, its current performance, and the total number of long-pulse target shots to date.

On-target 3ω energies have been limited by the laser-damage resistance of the installed 3ω transmissive optics.[3] Effort is underway to achieve OMEGA EP's long-pulse–design capability by procuring 3ω optics with greater laser-damage resistance. The current 3ω transport optics have been preconditioned to mitigate 3ω laser-induced damage growth to a fluence of 4 J/cm^2 (3-ns Gaussian pulse),[4] and it is anticipated that new processing methods[5] applied to newly procured 3ω optics may provide up to a factor-of-2 increase in damage threshold.[6]

Owing to the current fluence limitation, OMEGA EP must operate in a regime where both the beamline amplifiers and the frequency-conversion crystals are not highly saturated, making the 3ω near-field beam structure very sensitive to small changes in the injected beam quality. Several methods to improve the near-field beam profile have been pursued and are described in the next section.

The sensitivity to laser front-end performance necessitates significant effort and care to avoid exceeding the established fluence limit. To maintain a high level of operational efficiency, simulation tools have been developed that predict the 3ω near-field beam-fluence distribution and on-target energy using the preamplified injected near-field beam that is measured during pre-shot qualification. During shot operations, these tools have

Table 125.III: OMEGA EP long-pulse beamline performance.

Design	Current	Total long-pulse shots through FY10
2.5 kJ (t = 1 ns) 6.5 kJ (t = 10 ns)	1.0 kJ (t = 1 ns) 3.0 kJ (t = 10 ns)	278

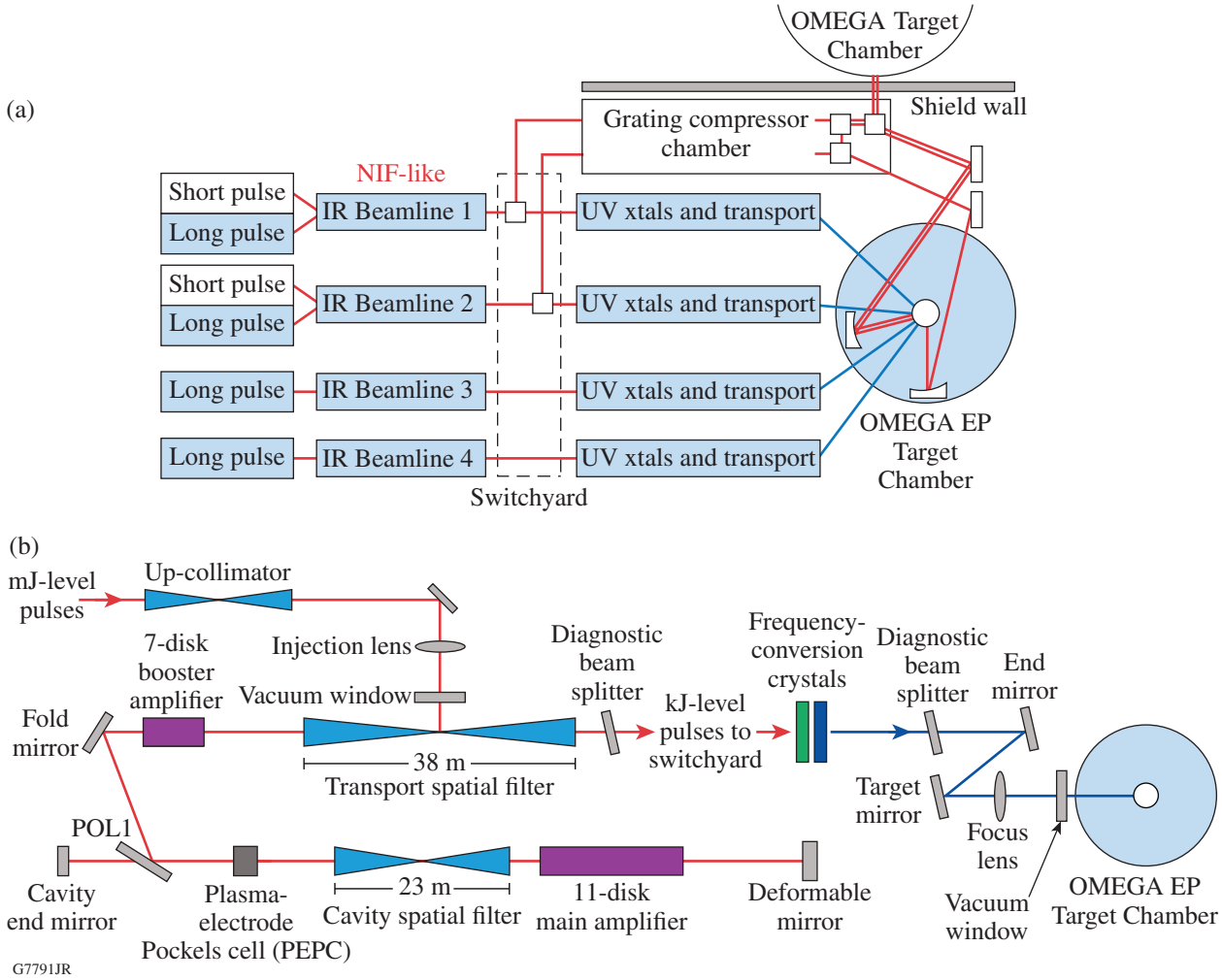

Figure 125.37
OMEGA EP Laser System configuration. (a) Beamlines 1 and 2 can be operated in either short-pulse or long-pulse mode, while Beamlines 3 and 4 are dedicated to long-pulse operation. (b) Each of the four beamlines uses a folded architecture and type-I/type-II frequency-conversion crystal design based on the NIF.

helped determine whether a user's energy requirements will be met without exceeding the 3ω damage threshold using the current injected beam profile, or whether more time should be given to alignment and qualification activities. The rapid prediction capability that these tools provide has helped to ensure safe fluence levels while maintaining high operational efficiency. These simulation tools are described in **Simulation Tools for Operations**, p. 41.

Near-Field Beam Improvements

Improved beam-shaping methods in both stages of apodization in the long-pulse front end have enhanced the efficiency of shot operations by providing consistently better beam profiles, therefore reducing the time required for pre-shot qualification. The following subsections describe (1) new apodizers that have been installed into both apodizing stages of Beamlines 3 and 4;[(a)] (2) a proof-of-concept experiment to smooth the 3ω near-field beam by detuning the FCC's; and (3) a programmable spatial light modulator (PSLIM), which will be installed into the front end of Beamlines 3 and 4 during FY11.

1. First-Stage Apodizer

Since there is only a small amount of saturation in the beamline, small changes in the regen output beam's profile can produce large changes in the 3ω beam. In practice, using the shape of the laser sources' regen output beam to precompensate for the approximately parabolic radial gain profile of the Nd:glass amplifiers has resulted in significant variations

[(a)]These upgrades will be implemented in the long-pulse front end of Beamlines 1 and 2 during FY11.

in 3ω beam quality. The day-to-day variations in regen beam quality and pointing make it necessary to adjust the centering of the regen beam profile into both the first-stage apodizer and the gain profile of the rod amplifier on shot day to optimize the 3ω beam profile, resulting in costly alignment delays. A new approach has been implemented that has significantly reduced the time required to optimize alignment. The regen output beam has been expanded at the location of the first apodizer to an approximately flat intensity distribution, and a new apodizer has been installed that shapes the beam from round to square and provides precompensation of the measured preamplifier radial gain using a binary mask.[7] The specified transmission profile combines a fourth-order polynomial fit to the measured small-signal radial gain with a square 40th-order super-Gaussian function. This has proven to be a much more robust design, providing better beam quality, greater ease of alignment, and greater reliability. Figure 125.38 shows that the measured transmission of the new apodizer matches the specified transmission within ~1%.

2. Second-Stage Apodizer

The first realization of the apodizer designed to precompensate beamline disk gain roll-off was a one-dimensional design [see Fig. 125.39(d)]. Following small-signal–gain measurements in Beamlines 3 and 4, an improved beam shaper that takes into account the beamline disk gain variations in two dimensions was designed and installed. The specified and measured transmission profiles for the new apodizer are shown in Figs. 125.39(a)–125.39(c). Figure 125.40 shows that a more uniform beam has been achieved after replacement of both front-end apodizers. The contrast of the beam, defined as the standard deviation of the fluence normalized to the average, was reduced from 16.8% to 12.6% with the installation of the new apodizers. The contrast was calculated over the 31-cm-square region shown overlaid on the beams in Fig. 125.40. The greater uniformity achieved within the overlaid region in Fig. 125.40(b) is attributed primarily to the first-stage apodizer, whereas the qualitative improvement in fill factor seen near the corners of the beam is attributed primarily to the second-stage apodizer.

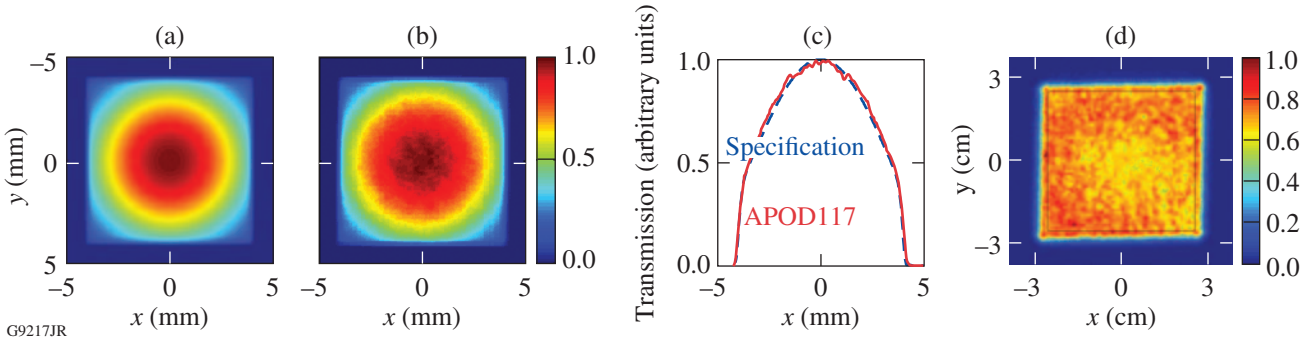

Figure 125.38
(a) Specified and (b) measured transmission of the new first-stage apodizer designed to precompensate the radial gain of the front-end Nd:glass amplifiers. Transmission lineouts are shown in (c) and the measured front-end output beam in (d).

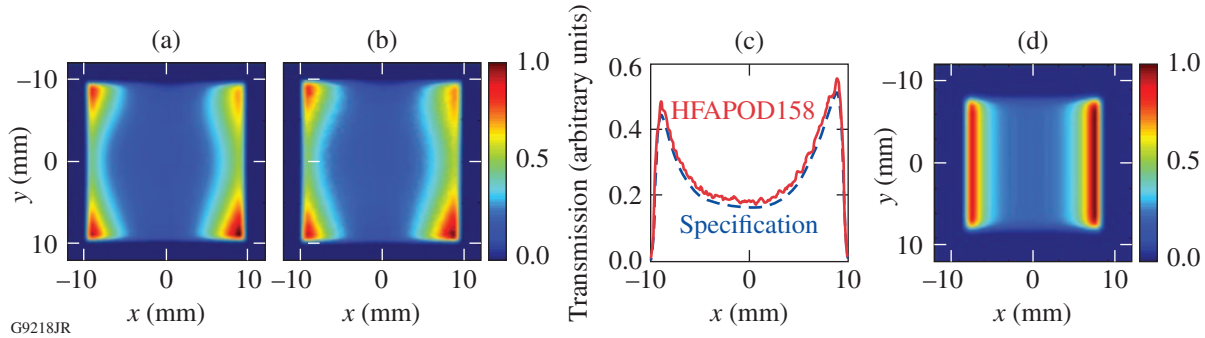

Figure 125.39
(a) Specified and (b) measured transmission of the new second-stage apodizer that precompensates the OMEGA EP beamline gain variation in two dimensions. Transmission lineouts are shown in (c). The previous one-dimensional apodizer design transmission is shown in (d).

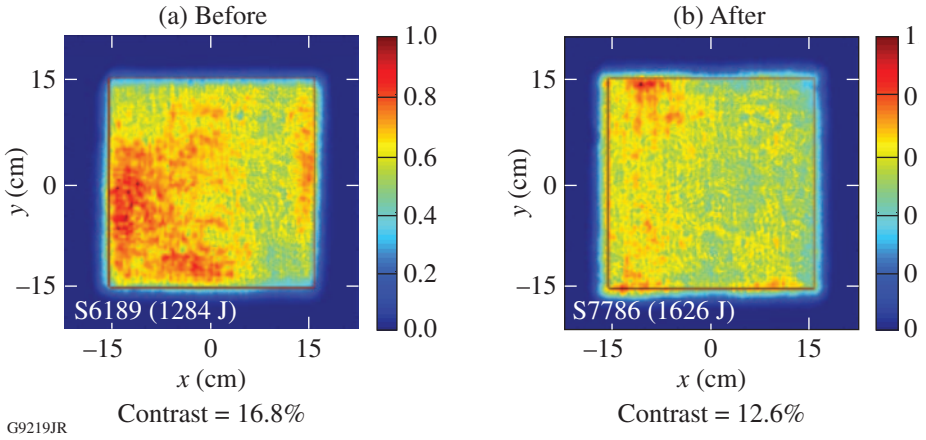

Figure 125.40
Normalized fluence of Beamline 4's 1ω output beams (a) before and (b) after installation of the new front-end apodizers. The contrast of the beam, defined as the standard deviation of the fluence normalized to the average and computed within the 31-cm × 31-cm area outlined in the figure, was reduced from 16.8% to 12.6% with the installation of the new apodizers.

3. UV Near-Field Beam Smoothing by FCC Detuning

Currently, the FCC's are angularly tuned to maximize the efficiency of the conversion process. When operated in this manner, the laser-damage thresholds of the current 3ω optics require that the 1ω laser intensity be maintained at a relatively low level (≤1 GW/cm^2). In this regime, small 1ω intensity variations produce large 3ω intensity variations, as shown in Fig. 125.41(a), causing the 3ω beam to be highly modulated. It has been proposed[8] that angularly detuning the FCC can reduce 3ω beam intensity modulations. Initial experiments on OMEGA EP have shown that by detuning the doubler crystal, the 3ω beam intensity modulation can be significantly reduced. The loss of conversion efficiency incurred by detuning the doubler is offset by increasing the 1ω energy into the FCC in order to maintain constant 3ω output energy [see Fig. 125.41(b)]. Measurements in Beamline 4 have shown a 13% reduction in peak 3ω fluence for the detuned FCC at nearly equivalent 3ω energy as the tuned FCC. Standard deviations of the 3ω beam fluence distributions were 21.2% and 14.7% for the tuned and detuned cases, respectively, indicating a significantly smoother beam for the detuned FCC, as shown in Fig. 125.42. This reduction in 3ω beam modulation should make it possible to deliver more energy to a target while maintaining peak 3ω intensities below the damage-threshold limit. To ensure that damage thresholds were not exceeded, this proof-of-concept experiment was performed at approximately half of the current 3ω energy limit for the 2-ns-square pulse shape used. The amount of increase in on-target energy that can be achieved will depend upon the reduction in peak fluence observed at energies approaching the 3ω damage threshold, which, in turn, will depend upon the level of saturation observed in the beamline. The utility of this beam-smoothing method on OMEGA EP will be explored in greater detail during FY11.

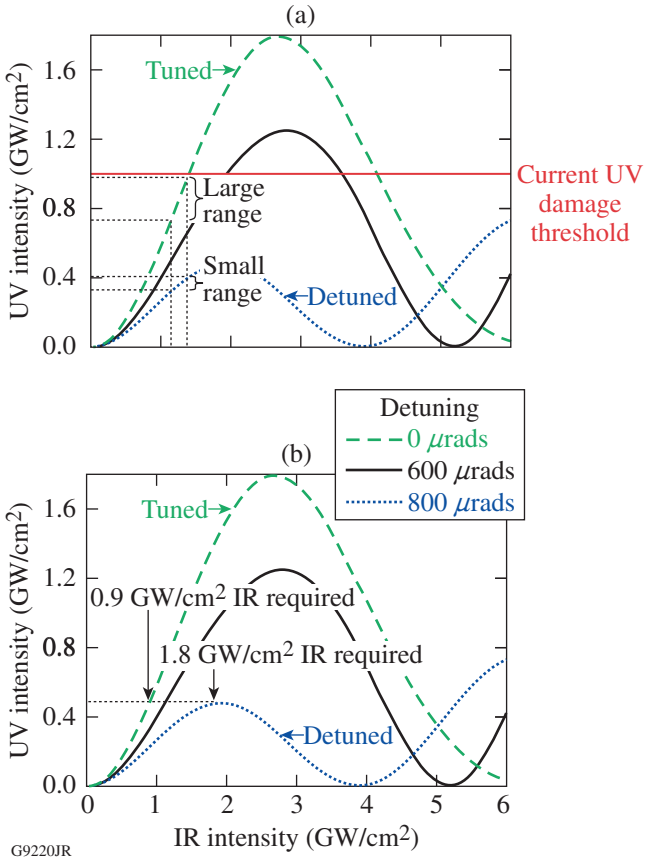

Figure 125.41
Simulated 3ω output versus 1ω input for the 11-mm–doubler, 9-mm–tripler OMEGA EP FCC design showing that (a) within the current operating regime of OMEGA EP, a detuned doubler can produce a smaller range of UV intensities for the same range of IR intensities than a tuned doubler; and (b) a detuned doubler requires more IR intensity to achieve the same UV intensity (or UV energy) as a tuned doubler.

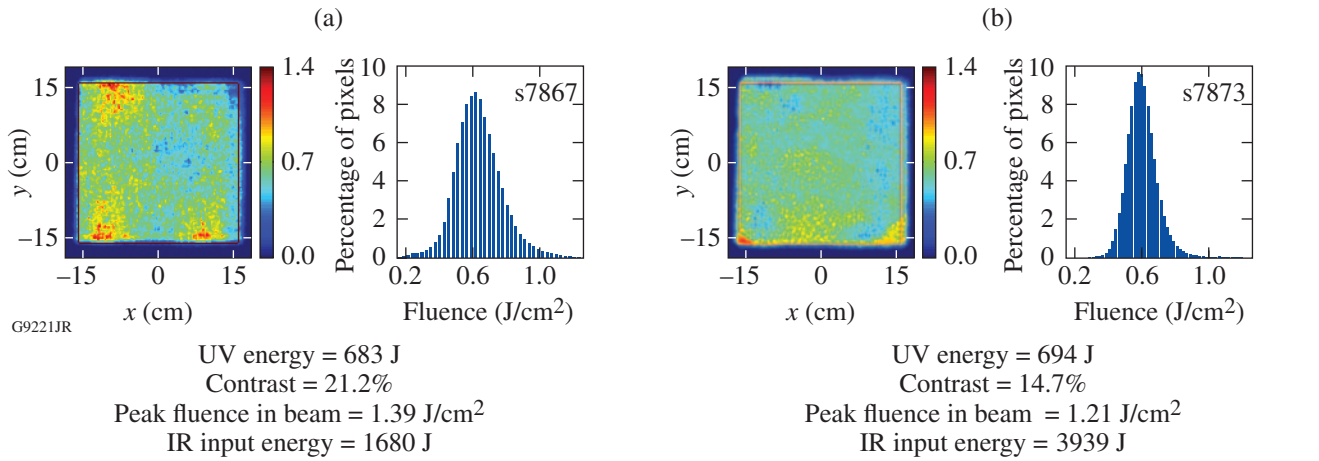

Figure 125.42
3ω near-field beams with (a) tuned and (b) detuned doubler measured on OMEGA EP Beamline 4 showing a significantly smoother beam for the detuned case.

4. Programmable Spatial Light Modulator (PSLIM)

A programmable spatial light modulator (PSLIM) will be installed into the front end of Beamlines 3 and 4 during FY11 to provide closed-loop correction of near-field beam amplitude. The PSLIM system shapes the laser beam's amplitude by using a liquid-crystal-on-silicon spatial light modulator that is based on an amplitude modulation carrier method.[9] It will be used primarily to improve the fill factor of the beam by the dynamic tuning of gain precompensation and to reduce near-field modulation by smoothing beam hot spots and edges.[10] Preliminary results for smoothing the beam at the location of the first apodizer in Beamline 3 are shown in Fig. 125.43.

Simulation Tools for Operations

The primary goal in the development of an operations simulation capability for OMEGA EP was to ensure UV system safety by predicting the 3ω peak fluence of an OMEGA EP beamline with high spatial resolution (1 k × 1 k) in a time frame of 10 min or less using measured data from the daily injection qualification shot. A rapid prediction capability ensures that system operators will be prepared to shoot again within a qualification shot cycle if additional alignment corrections are required. Because of the combined time-critical and high-spatial-resolution requirements, a simplified model was chosen and its performance was characterized against actual measurements. The IR portion of the model incorporates the previously measured, spatially dependent small-signal gain of the beamline disk amplifiers, with gain saturation accounted for using the Frantz–Nodvik equations.[11] A one-dimensional version of the model is also available for high-resolution, temporal pulse–shaping simulations. Physical processes that are not included are free-space propagation, wavefront aberrations, and high-frequency spatial noise. As will be shown, by characterizing the model against measurements of current system performance, the model can be used as an efficient tool to determine the maximum-allowable 3ω energy during

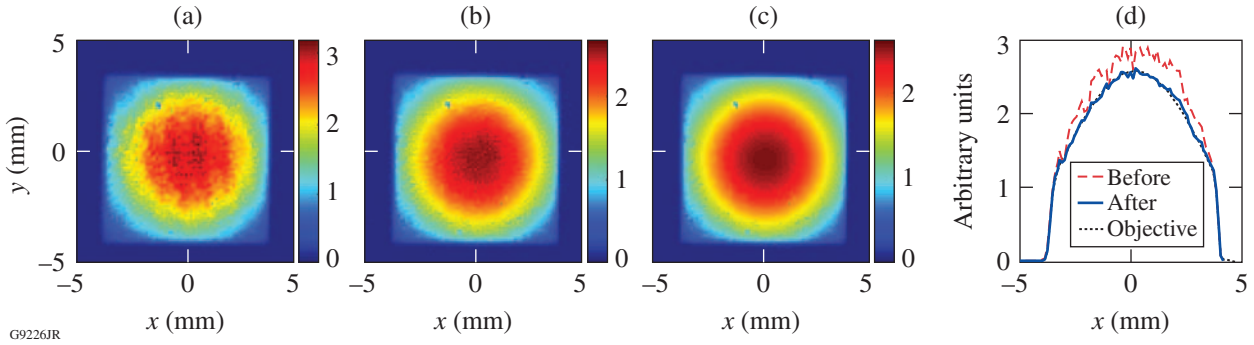

Figure 125.43
Initial results for fine-tuning the shape of the radial gain-precompensated beam using a programmable spatial light modulator (PSLIM) in the front end of Beamline 3: (a) before correction, (b) after correction. The objective map for the device is shown in (c) and lineouts in (d).

shot operations. Convergence of the model to the measured IR beamline energy is achieved by adjusting the per-disk loss to account for current system performance. The 3ω beam and pulse are simulated using spline interpolation of data that have been generated from prior frequency-conversion simulations. A pc-based, MATLAB framework was used to provide a seamless interface to pre-shot alignment and analysis tools and to provide an intuitive environment for rapid development, testing, and deployment. A multiple-core, distributed computing capability can optionally be used. Model output predictions include 1ω and 3ω beamline output energies, near-field beam-fluence distributions, and pulse shapes. The model also has backward prediction capability, which is used to perform shot setup based on the requested 3ω energy and pulse shape, and to calculate the maximum-allowable 3ω energy and associated injection energy on a shot day.

Figure 125.44 compares simulated and measured square pulses for the 1ω beamline output using the one-dimensional model. The agreement between the pulse shapes for N points in time is characterized by their root-mean-square (rms) difference:

$$\text{rms difference} = \sqrt{\frac{1}{N}\sum_{i=1}^{N}\left[\text{sim}(i) - \text{meas}(i)\right]^2}\,, \qquad (1)$$

which is equal to 4% for the pulses shown in Fig. 125.44(a). The simulations used the regen output pulse from an injection shot taken on the same day [see Fig. 125.44(b)]; therefore, the rms difference represents the model's predictive capability and the regen shot-to-shot pulse stability. The inset in Fig. 125.44(a) lists the simulated and measured beamline output energies, 3589 J and 3540 J, respectively. Figure 125.45 compares simulated and measured ramped pulse shapes for both the 1ω and 3ω beamline outputs. The rms difference in Fig. 125.45 is 3.6% for the 1ω pulse shape and 5.3% for the 3ω pulse shape. Table 125.IV shows that the measured and predicted beamline energies calculated using the pulse-shape prediction tool agree to within ~3%.

Simulated 1ω beamline output energies are compared with measurements in Fig. 125.46 for ~70 target shots taken during the third and fourth quarters of FY10. The simulations in Fig. 125.46 were performed using a 1-k × 1-k grid and 22 temporal slices and required ~7 min each. To avoid the additional computing time required for the temporal integration in the IR section of the beamline, a continuous-wave (cw) amplification model is also available. Figure 125.47(a) compares simulated, 1ω beamline output energies with measured energies using the cw model; Fig. 125.47(b) shows the corresponding 3ω on-target

Table 125.IV: Simulated and measured beamline output energies for Beamline 3 (shot 7799) using the pulse-shape–prediction tool. The regen pulse shape for a qualification shot taken on the same day was used in the simulation.

	Simulation	Measurement
IR (J)	1375	1416
UV on-target (J)	442	454

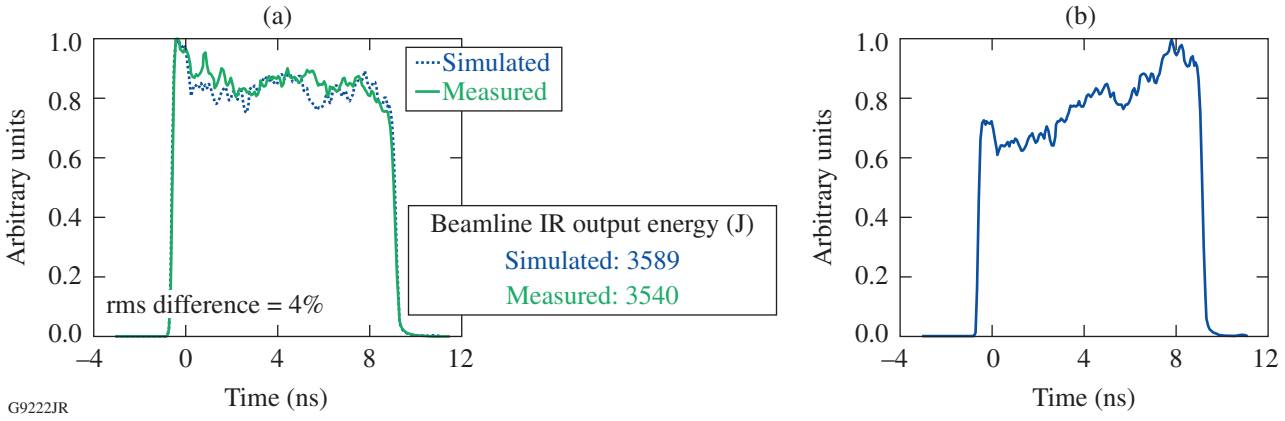

Figure 125.44
Simulated and measured ESG9901 square-pulse shapes are shown in (a) for the 1ω output of Beamline 4. Beamline energies and the rms difference between simulated and measured pulse shapes are given in the figure. Simulations used the regen output pulse shape shown in (b) for an injection shot taken on the same day.

energies. In this case, the 3ω simulations used measured IR beamline output-pulse shapes. The agreement between the simulations and measurements is within ~5%, although an ~5% systematic offset is apparent in the region between 2 to 3 kJ in Figs. 125.46 and 125.47(a) and between 1 to 1.2 kJ in Fig. 125.47(b). This is suspected to be caused by a temporary calibration drift in the energy diagnostic used for these shots. These results demonstrate the model's capability to accurately predict beamline energy and pulse shape using the measured qualification shot data.

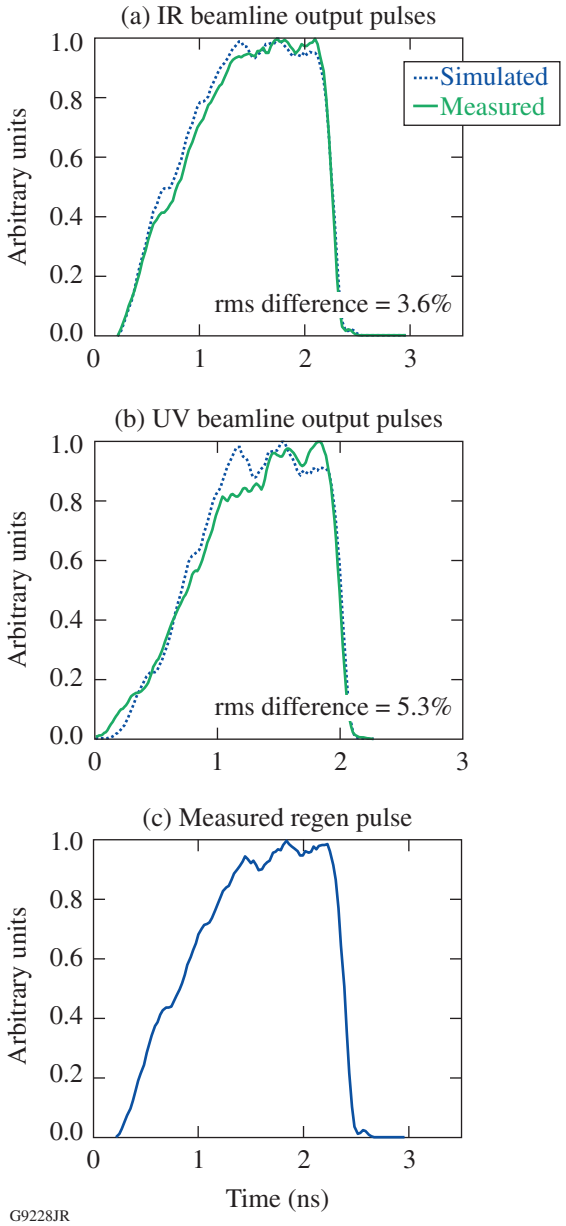

Figure 125.45
Simulated and measured ERM2001 ramped-pulse shapes are shown in (a) and (b) for Beamline 3's 1ω and 3ω outputs, respectively. The rms differences between simulated and measured pulse shapes are given in the figure. Simulations used the regen output-pulse shape shown in (c) for an injection shot taken on the same day.

Simulated 3ω peak fluences for shots on OMEGA EP using a 1-k × 1-k grid and 22 temporal slices are compared with their corresponding measured values in Fig. 125.48. The simulated values are, on average, ~9% below the measurements and are generally well within 20%. The difference between the 9% and 20% levels corresponds to the 2-σ distance for the fluence distribution formed by the difference between simulated and measured values. The systematic offset of the simulated peak fluence from the measured values suggests that allowable 3ω energies can be safely established using simulations that provide peak fluences less than or equal to 80% of the 3ω damage threshold. For OMEGA EP users requesting maximum 3ω energy on the first target shot of the day, the maximum-allowable energy is calculated in a two-step process: Prior to shot day, the 3ω energy limit is established based on the amount of modulation observed in the most recently measured 3ω near-field beam. This enables users to specify the entire laser configuration well in advance of the shot. On shot day, the maximum-allowable 3ω energy is calculated using the measured injected near-field beam to give a simulated peak fluence that is equal to 80% of the 3ω damage threshold. Simulations on shot day account for (1) changes in the injected near-field beam and (2) possible differences between the pre-shot-day and current-shot-day beamline configurations that may affect

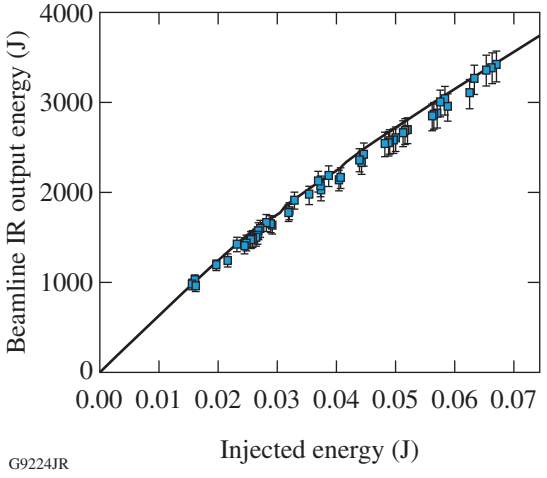

Figure 125.46
Simulated (line) and measured 1ω output energy versus injected energy of Beamline 4 with 16 laser slabs (9/7 main/booster amplifier configuration). Measurements represent the approximately 70 target shots taken during the third and fourth quarters of FY10.

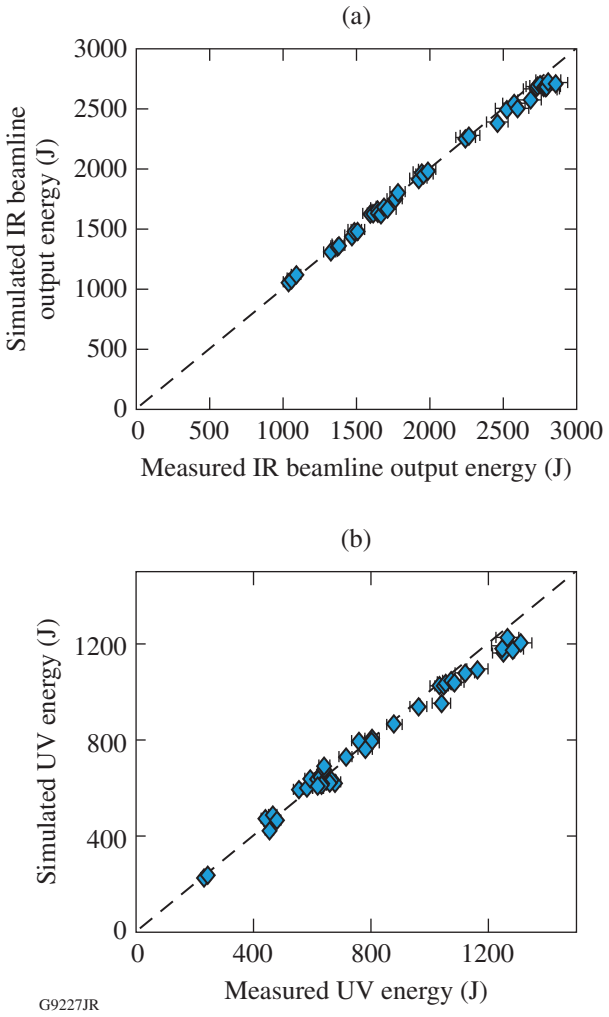

Figure 125.47
Simulated energies using the cw IR and UV beamline models versus measured energies: (a) 1ω Beamline 3 output and (b) corresponding 3ω on-target energy. The dashed line with slope of 1 is shown for reference.

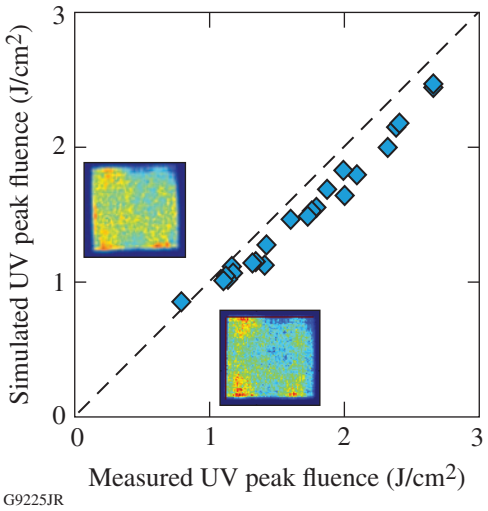

Figure 125.48
3ω peak fluence simulated by using the measured injected near-field beam is plotted against the corresponding measured peak fluence for several OMEGA EP target shots. A simulated and corresponding measured 3ω beam is also shown for one case. Simulated values were ~9% below measurements, on average (dashed line with slope of 1 is shown for reference). By characterizing the model's predictive capability, high-resolution, end-to-end beamline simulations were performed and facility direction provided to operators within a qualification shot cycle.

UV near-field modulation. This two-step process provides a shot-ready laser configuration and ensures that 3ω damage thresholds are not exceeded. Typically, only small adjustments to the injection-energy throttle setting are required to achieve, on the first shot, measured 3ω peak fluences that are between 85% and 95% of the 3ω damage threshold. Notably, no significant damage has been observed to date in the long-pulse section of the OMEGA EP beamlines.

Summary

We have described several performance enhancements in the long-pulse section of OMEGA EP that have resulted in better beam quality, greater reliability, and improved efficiency during shot operations. The sensitivity to front-end, near-field beam quality that results from operation in a regime of low saturation has been reduced using new apodizer designs. These designs have significantly improved the near-field beam profile and reduced the time required to qualify the injected beam. Other methods to reduce beam modulation, such as FCC detuning and the implementation of a PSLIM, are also being pursued. We have described simulation tools used during shot operations that have provided rapid and accurate predictions of beamline performance, ensuring that laser-damage thresholds are not exceeded and providing facility direction to operators within a qualification shot cycle. Higher-damage-threshold UV transport optics have also been procured. Higher energies will allow for greater saturation, greater levels of beam smoothing, and greater on-target energy for a given peak fluence.

ACKNOWLEDGMENT

The authors thank the OMEGA EP operations team for their contributions to the measurements reported here. This work was supported by the U.S. Department of Energy Office of Inertial Confinement Fusion under Cooperative Agreement No. DE-FC52-08NA28302, the University of Rochester, and the New York State Energy Research and Development Authority. The support of DOE does not constitute an endorsement by DOE of the views expressed in this article.

REFERENCES

1. J. H. Kelly, L. J. Waxer, V. Bagnoud, I. A. Begishev, J. Bromage, B. E. Kruschwitz, T. J. Kessler, S. J. Loucks, D. N. Maywar, R. L. McCrory, D. D. Meyerhofer, S. F. B. Morse, J. B. Oliver, A. L. Rigatti, A. W. Schmid, C. Stoeckl, S. Dalton, L. Folnsbee, M. J. Guardalben, R. Jungquist, J. Puth, M. J. Shoup III, D. Weiner, and J. D. Zuegel, J. Phys. IV France **133**, 75 (2006).

2. T. Alger *et al.*, Lawrence Livermore National Laboratory, Livermore, CA, Report UCRL-ID-132680 (NIF-0014142), NTIS Order No. DE2002-791837 (1999). (Copies may be obtained from the National Technical Information Service, Springfield, VA 22161.)

3. Estimated to be 4 J/cm^2 with a 3-ns Gaussian pulse.

4. I. L. Bass *et al.*, in *High-Power Laser Ablation VI*, edited by C. R. Phipps (SPIE, Bellingham, WA, 2006), Vol. 6261, p. 62612A.

5. T. I. Suratwala *et al.*, "HF-Based Etching Processes for Improving Laser Damage Resistance of Fused Silica Optical Surfaces," to be published in the Journal of the American Ceramic Society.

6. See Fig. 1 of Ref. 5.

7. C. Dorrer and J. D. Zuegel, J. Opt. Soc. Am. B **24**, 1268 (2007).

8. R. S. Craxton, IEEE J. Quantum Electron. **QE-17**, 1771 (1981).

9. V. Bagnoud and J. D. Zuegel, Opt. Lett. **29**, 295 (2004).

10. S.-W. Bahk, E. Fess, B. E. Kruschwitz, and J. D. Zuegel, Opt. Express **18**, 9151 (2010).

11. L. M. Frantz and J. S. Nodvik, J. Appl. Phys. **34**, 2346 (1963).